

1  
2  
3  
4  
5  
6  
7  
8  
9  
10  
11  
12  
13  
14  
15  
16  
17  
18  
19  
20  
21  
22  
23  
24  
25  
26  
27  
28  
29  
30  
31  
32  
33  
34  
35  
36  
37  
38  
39  
40  
41  
42  
43  
44  
45  
46  
47  
48  
49  
50  
51  
52

## Title

Quantitative Mass Spectrometry Analysis of Cerebrospinal Fluid Protein Biomarkers in Alzheimer’s Disease

## Authors

Caroline M. Watson<sup>1</sup>, Eric B. Dammer<sup>1</sup>, Lingyan Ping<sup>1</sup>, Duc M. Duong<sup>2</sup>, Erica Modeste<sup>1</sup>, E. Kathleen Carter<sup>2</sup>, Erik C. B. Johnson<sup>1</sup>, Allan I. Levey<sup>1\*</sup>, James J. Lah<sup>1\*</sup>, Blaine R. Roberts<sup>1,2</sup>, and Nicholas T. Seyfried<sup>1,2\*</sup>

## Affiliations

1. Department of Neurology, Emory University School of Medicine  
2. Department of Biochemistry, Emory University School of Medicine  
corresponding author(s): Nicholas T. Seyfried, PhD ([nseyfri@emory.edu](mailto:nseyfri@emory.edu)); James J. Lah, MD, PhD. ([jlal@emory.edu](mailto:jlal@emory.edu)); Allan I Levey, MD, PhD. ([alevey@emory.edu](mailto:alevey@emory.edu))

## Abstract

Alzheimer’s disease (AD) is the most common form of dementia, with cerebrospinal fluid (CSF)  $\beta$ -amyloid ( $A\beta$ ), total Tau, and phosphorylated Tau providing the most sensitive and specific biomarkers for diagnosis. However, these diagnostic biomarkers do not reflect the complex changes in AD brain beyond amyloid (A) and Tau (T) pathologies. Here, we report a selected reaction monitoring mass spectrometry (SRM-MS) method with isotopically labeled standards for relative protein quantification in CSF. Biomarker positive (AT+) and negative (AT-) CSF pools were used as quality controls (QCs) to assess assay precision. We detected 62 peptides (51 proteins) with an average CV of ~13% across 30 QCs and 133 controls (cognitively normal, AT), 127 asymptomatic (cognitively normal, AT+) and 130 symptomatic AD (cognitively impaired, AT+). Proteins that could distinguish AT+ from AT- individuals included SMOC1, GDA, 14-3-3 proteins, and those involved in glycolysis. Proteins that could distinguish cognitive impairment were mainly neuronal proteins (VGF, NPTX2, NPTXR, and SCG2). This demonstrates the utility of SRM-MS to quantify CSF protein biomarkers across stages of AD.

## Background & Summary

Alzheimer’s disease (AD) affects more than 45 million people worldwide, making it the most common neurodegenerative disease<sup>1</sup> (<https://www.alz.org/media/Documents/alzheimers-facts-and-figures-2019-r.pdf>; <https://www.alzint.org/u/WorldAlzheimerReport2015.pdf>). AD biomarker research has predominately focused on  $\beta$ -amyloid ( $A\beta$ ) and Tau, as these proteins reflect pathological  $A\beta$  plaques and tau neurofibrillary tangles (NFT), respectively, in AD<sup>2,3</sup>. Although  $A\beta$  and Tau are the most sensitive and specific CSF biomarkers for diagnosis<sup>4,5</sup> these two proteins do not reflect the heterogenous and complex changes in AD brain<sup>6,7</sup>. Furthermore, failed clinical trials of  $A\beta$ -based therapeutic approaches highlight the complexity of AD and the need for additional biomarkers to fully illustrate pathophysiology for advancements in diagnostic profiling, disease monitoring, and treatments<sup>1,7</sup> (<https://www.alz.org/media/Documents/alzheimers-facts-and-figures-2019-r.pdf>; <https://www.alzint.org/u/WorldAlzheimerReport2015.pdf>).

Considering the diagnostic challenges related to the overlapping pathologies of neurodegenerative diseases, AD biomarkers that represent diverse pathophysiological

53 changes could facilitate an early diagnosis, predict disease progression, and enhance the  
54 understanding of neuropathological changes in AD<sup>1</sup>. AD has a characteristic pre-clinical or  
55 asymptomatic period (AsymAD) where individuals have AD neuropathology in the absence of  
56 clinical cognitive decline<sup>3,8,9</sup>. Thus, biomarkers for the prodromal phase of AD that can begin  
57 changing years or decades before signs of cognitive impairment, would be valuable for disease  
58 intervention, clinical trial stratification, and monitoring drug efficacy.

59  
60 Proteins are the proximate mediators of disease, integrating the effects of genetic, epigenetic,  
61 and environmental factors<sup>7,10</sup>. Network proteomic analysis has emerged as a valuable tool for  
62 organizing complex unbiased proteomic data into groups or “modules” of co-expressed  
63 proteins that reflect various biological functions, i.e., systems biology<sup>11-14</sup>. The direct proximity  
64 of CSF to the brain presents a strong rationale to integrate the brain and CSF proteomes to  
65 increase the pathophysiological diversity among biofluid biomarkers of AD<sup>5,15</sup>. We recently  
66 integrated a human AD brain proteomic network with a CSF proteome differential expression  
67 analysis and revealed approximately 70% of the CSF proteome overlapped with the brain  
68 proteome<sup>16</sup>. Nearly 300 CSF proteins were identified as significantly altered between control  
69 and AD samples, representing predominately neuronal, glial, vasculature and metabolic  
70 pathways, creating an excellent list of candidates for further quantification and validation.

71  
72 Here, we developed a high-throughput targeted selected reaction monitoring-based mass  
73 spectrometry (SRM-MS) assay<sup>17</sup> to quantify and validate reliably detected CSF proteins in  
74 healthy individuals and individuals with asymptomatic or symptomatic AD for staging AD  
75 progression. We evaluated 200+ tryptic peptides that were selected using a data-driven  
76 approach from the integrated brain-CSF proteome network analysis. We selected peptides  
77 with differential abundance in AD CSF observed in >50 percent of case samples by discovery  
78 proteomics<sup>16</sup> for synthesis as crude heavy standards. We used two pooled CSF reference  
79 standards to determine which peptides were reliably detected in CSF matrix. We reproducibly  
80 detected and reliably quantified 62 tryptic peptides from 51 proteins in 390 clinical samples  
81 and 30 pooled reference standards. Furthermore, using a combination of differential  
82 expression and receiver operating curve (ROC) analyses we found CSF proteins that can best  
83 discriminate stages of AD progression. Collectively, these data highlight the utility of a high  
84 throughput SRM-MS approach to quantify biomarkers associated with AD that ultimately hold  
85 promise for monitoring disease progression, stratifying patients for clinical trials, and  
86 measuring therapeutic response. Future studies will be necessary to assess the diagnostic and  
87 predictive utility of our CSF peptide SRM panel against gold-standard CSF (amyloid, tau and  
88 pTau) and imaging AD biomarkers in larger prospective patient cohorts.

89  
90

## 91 **Methods**

92  
93

### 94 **Reagents and materials**

94 Heavy labeled peptides (Thermo PEPotec SRM Peptide Libraries; Grade 2; crude as  
95 synthesized), trypsin, mass spectrometry grade, trifluoroacetic acid (TFA), foil heat seals (AB-  
96 0757), and low-profile square storage plates (AB-1127) were purchased from ThermoFisher  
97 Scientific (Waltham, MA). Lysyl endopeptidase (Lys-C), mass spectrometry grade was bought  
98 from Wako (Japan); sodium deoxycholate, CAA (chloroacetamide), TCEP (tris-2(-carboxyethyl)-  
99 phosphine), and triethylammonium hydrogen carbonate buffer (TEAB) (1 M, pH 8.5) were  
100 obtained from Sigma (St. Louis, MO). Formic acid (FA), 0.1% FA in acetonitrile, 0.1% FA in  
101 water, methanol, and sample preparation V-bottom plates (Greiner Bio-One 96-well  
102 Polypropylene Microplates; 651261) are from Fisher Scientific (Pittsburgh, PA). Oasis PRiME  
103 HLB 96-well, 30mg sorbent per well, solid phase extraction (SPE) cleanup plates were from  
104 Waters Corporation (Milford, MA).

105

106

### 107 **Pooled CSF as quality controls**

108 Two pools of CSF were generated based on A $\beta$ (1-42), total Tau, and pTau181 levels to create  
109 AD-positive (AT+) and AD-negative (AT-) quality control standards. Each pool consisted of  
110 approximately 50 mL of CSF by combining equal volumes of CSF selected from well  
111 characterized samples (~45 unique individuals per pool) from the Emory Goizueta Alzheimer's  
112 Disease Research Center (GADRC) and Emory Healthy Brain Study (EHBS). All research  
113 participants provided informed consent under protocols approved by the Institutional Review  
114 Board (IRB) at Emory University. CSF was collected by lumbar puncture and banked according  
115 to 2014 ADC/NIA best practices guidelines ([https://www.alz.washington.edu/Biospecimen  
116 TaskForce.html](https://www.alz.washington.edu/BiospecimenTaskForce.html)). AD biomarker status for individual cases was determined on the Roche  
117 Elecsys<sup>®</sup> immunoassay platform<sup>18-20</sup>; the average CSF biomarker value is reported in  
118 parentheses. The control CSF pool (AT-) was comprised of cases with relatively high levels of  
119 A $\beta$ (1-42) (1457.3 pg/mL) and low total Tau (172.0 pg/mL) and pTau181 (15.1 pg/mL). In  
120 contrast, the AD pool (AT+) was comprised of cases with low levels of A $\beta$ (1-42) (482.6 pg/mL)  
121 and high total Tau (341.3 pg/mL) and pTau181 (33.1 pg/mL). The quality control (QC) pools  
122 were processed and analyzed identically to the CSF clinical samples reported.

123

### 124 **Clinical characteristics of the cohort**

125 Human cerebrospinal fluid (CSF) samples from 390 individuals including 133 healthy controls,  
126 130 patients with symptomatic AD, and 127 asymptomatic AD patients (cognitively normal but  
127 AD biomarker positive) were obtained from Emory's GADRC and EHBS (**Fig. 1 and Table 1**). All  
128 symptomatic individuals were diagnosed by expert clinicians in the ADRC and Emory Cognitive  
129 Neurology Program, who are subspecialty trained in Cognitive and Behavioral Neurology,  
130 following extensive clinical evaluations including detailed cognitive testing, neuroimaging, and  
131 laboratory studies. CSF samples were selected to balance for age and sex (**Table 1**). For  
132 biomarker measurements, CSF samples from all individuals were assayed for A $\beta$ (1-42), total  
133 Tau, and pTau using the Roche Diagnostics Elecsys<sup>®</sup> immunoassay platform<sup>18-20</sup>. The cohort  
134 characteristics are summarized in **Fig. 1 and Table 1**. Compared to our previous CSF  
135 studies<sup>14,16,21</sup>, there is minimal overlap with 329 of the 390 CSF samples (~84%) unique to this  
136 study. Samples were stratified into controls, AsymAD, and AD based on Tau and Amyloid  
137 biomarkers status and cognitive score from the Montreal Cognitive Assessment (MoCA). All  
138 case metadata including disease state, age, sex, race, apolipoprotein (ApoE) genotype, MoCA  
139 scores, and biomarkers measurements were deposited on Synapse<sup>22</sup>.

140

### 141 **Peptide selection and selected reaction monitoring assay**

142 We harnessed both deep discovery and single-shot tandem mass tag (ssTMT) peptide data  
143 from CSF proteomics<sup>14,16</sup>. Here, we prioritized peptides for SRM validation that i) had one or  
144 more spectral match, ii) were differentially abundant (AD versus control) iii) or that mapped  
145 to proteins within brain-based biological panels that differed in AD<sup>16</sup>. Ultimately, we  
146 nominated 200+ peptides for synthesis as crude heavy standards. The heavy peptides  
147 contained isotopically labeled C-terminal lysine or arginine residues (<sup>13</sup>C, <sup>15</sup>N) for each tryptic  
148 peptide. Based on the crude heavy peptide signal, the peptides were pooled to achieve total  
149 area signals  $\geq 1 \times 10^5$  in CSF matrix. The transition lists were created in Skyline-daily software  
150 (version 21.2.1.455)<sup>23,24</sup>. An in-house spectral library was created in Skyline based on tandem  
151 mass spectra from CSF samples. Skyline parameters were specified as: trypsin enzyme, Swiss-  
152 Prot background proteome, and carbamidomethylation of cysteine residues (+57.02146 Da)  
153 as fixed modifications. Isotope modifications included: <sup>13</sup>C<sub>6</sub><sup>15</sup>N<sub>4</sub> (C-term R) and <sup>13</sup>C<sub>6</sub><sup>15</sup>N<sub>2</sub> (C-term  
154 K). The top ten fragment ions that matched the criteria (precursor charges: 2; ion charges 1,  
155 2; ion types: y, b) were selected for scrutiny. The top 5-7 transitions per heavy precursor were  
156 selected by manual inspection of the data in Skyline and scheduled transition lists were

157 created for collision energy optimization. Collision energies were optimized for each  
158 transition; the collision energy was ramped around the predicted value in 3 steps on both  
159 sides, in 2V increments<sup>25</sup>. The selected transitions were tested in real matrix spiked with the  
160 heavy peptide mixtures. The three best transitions per precursor were selected by manual  
161 inspection of the data in Skyline and one scheduled transition list was created for the final  
162 assays. A list of transitions used in this study is deposited on Synapse<sup>22</sup>.

163

#### 164 **Preparation of CSF for mass spectrometric analysis**

165 All CSF samples were blinded and randomized. Each CSF sample was thawed and aliquoted  
166 into sample preparation V-bottom plates that also included quality controls. Each sample and  
167 quality control were processed independently in parallel. Crude CSF (50  $\mu$ L) was reduced,  
168 alkylated, and denatured with tris-2(-carboxyethyl)-phosphine (5 mM), chloroacetamide (40  
169 mM), and sodium deoxycholate (1%) in triethylammonium bicarbonate buffer (100 mM) in a  
170 final volume of 150  $\mu$ L. Sample plates were heated at 95°C for 10 min, followed by a 10-min  
171 cool down at room temperature while shaking on an orbital shaker (300 rpm)<sup>26</sup>. CSF proteins  
172 were digested with Lys-C (Wako; 0.5  $\mu$ g; 1:100 enzyme to CSF volume) and trypsin (Pierce; 5  
173  $\mu$ g; 1:10 enzyme to CSF volume) overnight in a 37°C oven. After digestion, heavy labeled  
174 standards for relative quantification (15  $\mu$ L per 50  $\mu$ L CSF) were added to the peptide solutions  
175 followed by acidification to a final concentration of 0.1% TFA and 1% FA (pH  $\leq$  2). Sample plates  
176 were placed on an orbital shaker (300 rpm) for at least 10 minutes to ensure proper mixing.  
177 Plates were centrifuged (4680 rpm) for 30 minutes to pellet the precipitated surfactant.  
178 Peptides were desalted with Oasis PRiME HLB 96-well, 30mg sorbent per well, solid phase  
179 extraction (SPE) cleanup plates from Waters Corporation (Milford, MA) using a positive  
180 pressure system. Each SPE well was conditioned (500  $\mu$ L methanol) and equilibrated twice  
181 (500  $\mu$ L 0.1% TFA) before 500  $\mu$ L 0.1% TFA and supernatant were added. Each well was washed  
182 twice (500  $\mu$ L 0.1% TFA) and eluted twice (100  $\mu$ L 50% acetonitrile/0.1% formic acid). All  
183 eluates were dried under centrifugal vacuum and reconstituted in 50  $\mu$ L mobile phase A (0.1%  
184 FA in water) containing Promega 6  $\times$  5 LC-MS/MS Peptide Reference Mix (50 fmol/ $\mu$ L; Promega  
185 V7491).

186

#### 187 **Liquid chromatography-tandem mass spectrometry (LC-MS/MS)**

188 Peptides were analyzed using a TSQ Altis Triple Quadrupole mass spectrometer (Thermo  
189 Fisher Scientific). Each sample was injected (20  $\mu$ L) using a 1290 Infinity II system (Agilent) and  
190 separated on an AdvanceBio Peptide Map Guard column (2.1 $\times$ 5mm, 2.7  $\mu$ m, Agilent)  
191 connected to AdvanceBio Peptide Mapping analytical column (2.1 $\times$ 150mm, 2.7  $\mu$ m, Agilent).  
192 Sample elution was performed over a 14-min gradient using mobile phase A (MPA; 0.1% FA in  
193 water) and mobile phase B (MPB; 0.1% FA in acetonitrile) with flow rate at 0.4 mL/min. The  
194 gradient was from 2% to 24% MPB over 12.1 minutes, then from 24% to 80% over 0.2 min and  
195 held at 80% B for 0.7 min. The mass spectrometer was set to acquire data in positive-ion mode  
196 using selected reaction monitoring (SRM) acquisition. Positive ion spray voltage was set to  
197 3500 V for the Heated ESI source. The ion transfer tube and vaporizer temperatures were set  
198 to 325°C and 375°C, respectively. SRM transitions were acquired at Q1 resolution 0.7 FWHM,  
199 Q2 resolution 1.2 FWHM, CID gas 1.5 mTorr, 0.8 s cycle time.

200

#### 201 **Data analysis**

202 Raw files from Altis TSQ were uploaded to Skyline-daily software (version 21.2.1.455), which  
203 was used for peak integration and quantification by peptide ratios. QC SRM data were  
204 manually evaluated in Skyline by assessing retention time reproducibility, matching light and  
205 heavy transitions using Ratio Dot Product, and determining the peptide ratio precision using  
206 CV by QC condition. If Skyline could not automatically pick a consistent peak due to  
207 interference in the light transitions the peptide was removed from the analysis. Transition  
208 profiles were checked to insure the heavy and light transition profiles matched using the Ratio



209 Dot Product value in Skyline. The Ratio Dot Product (1 = exact match) is a measure of whether  
210 the transition peak areas in the two label types are in the same ratio to each other. The average  
211 Ratio Dot Product value for each peptide was >0.90 for each QCs. If the retention time or Ratio  
212 Dot Product were outside of the expected range for a peptide in a few samples, the peaks  
213 were checked individually and adjusted as necessary. Total area ratios for each peptide were  
214 calculated in Skyline by summing the area for each light (3) and heavy (3) transition and  
215 dividing the light total area by the heavy total area. The Total Area Ratio CV was assessed using  
216 Skyline and the peptide was removed from the analysis if the CV>20% by QC condition. Next,  
217 the individual CSF samples were analyzed in a blinded fashion. We used the total area ratios  
218 (peptide ratios) for each targeted peptide in each sample and QC analysis; therefore, there are  
219 no missing values in the Data Matrix on Synapse. The raw data files and Skyline file have been  
220 deposited on Synapse<sup>22</sup>.

221

## 222 **Statistical analyses**

223 We used Skyline-daily software (version 21.2.1.455) and GraphPad Prism (version 9.4.1)  
224 software to calculate means, medians, standard deviations, and coefficients of variations<sup>24</sup>.  
225 Peptide abundance ratios were log<sub>2</sub>-transformed, and zero values were imputed as one-half  
226 the minimum nonzero abundance measurement. Then, one-way ANOVA with Tukey *post hoc*  
227 tests for significance of the paired groupwise differences across diagnosis groups was  
228 performed in R (version 4.0.2) using a custom calculation and volcano plotting framework  
229 implemented and available as an open-source set of R functions documented further on  
230 <https://www.github.com/edammer/parANOVA>. T test p values and Benjamini-Hochberg FDR  
231 for these are reported for two total group comparisons, as was the case for AT+ versus AT-  
232 peptide mean difference significance calculations. Receiver-operating characteristic (ROC)  
233 analysis was performed in R (version 4.0.2) with a generalized linear model binomial fit of each  
234 set of peptide ratio measurements to the binary case diagnosis subsets AD/Control,  
235 AsymAD/Control, and AD/AsymAD using the pROC package implementing ROC curve plots,  
236 and calculations of AUC and AUC DeLong 95% confidence interval. Additional ROC curve  
237 characteristics including sensitivity, specificity, and accuracy were calculated with the  
238 reportROC R package. Robustness of the ROC calculations of AUC were confirmed using k-fold  
239 cross validation (k=10 folds, with each fold containing case subsets with equal distributions of  
240 the binary outcome) implemented using the cvAUC R package functions for calculating cross-  
241 validated AUC (cvAUC), and confidence interval on pooled predictions, and these calculations  
242 were consistently within 1 percent of AUC as calculated using a single calculation on the full  
243 data (data not shown). Venn diagrams were generated using the R vennEuler package, and the  
244 heatmap was produced using the R pheatmap package/function. R boxplot function output  
245 was overlaid with beeswarm-positioned individual measurement points using the R beeswarm  
246 package. Pearson correlations of SRM peptide measurements to immunoassay measurements  
247 of A $\beta$ (1-42), total Tau, phospho-T181 Tau, and the ratio of total Tau/ A $\beta$  were performed using  
248 the corAndPvalue WGCNA function in R. Correlation scatterplots were generated using the  
249 verboseScatterplot WGCNA function.

250

## 251 **Data Records**

252

253 All files have been deposited on Synapse<sup>22</sup>. The data folder contains sample traits, transition  
254 details, the peptide ratio data matrix, transition ratios, and protein details. The Metadata file  
255 contains the available traits for each sample analyzed including: SampleID – Internal Sample  
256 Identifier; Age(years) – Deidentified Age in years; Sex – Binary Sex; Race – self identified race;  
257 Educ – formal years of education; MoCA – Montreal Cognitive Assessment Score ranging from  
258 0-30; APOE status – APOE genotype; A $\beta$ 42, tTau, pTau – as measured in CSF by Roche Elecsys®  
259 immunoassay platform; tTau:A $\beta$ 42 – ratio of tTau/ A $\beta$ 42; SampleRunOrder – the order the  
260 samples were acquired; Condition – the Control/AsymAD/AD group used in the analysis. The

261 DataMatrix file contains peptide ratio data for each sample. Data file names are list in the top  
262 row of the DataMatrix: AT+ QC samples begin with AD\_; AT- QC samples begin with CTL\_  
263 Individual samples can be mapped back to the Metadata using the sample run order (Sxxx) or  
264 SampleID (\_xxxx); Plate/box and well position also defined in the file name (\_Bx\_Axx). The  
265 MS RAW files folder contains all mass spectrometry raw files (N=423) from both quality control  
266 replicates and clinical samples. The Skyline quantification folder contains the Skyline file that  
267 was used to report the peptide ratios, calculate CVs and means, and ratio dot product.

268

## 269 **Technical Validation**

270

### 271 **Assessing peptide precision using pooled CSF quality control (QC) standards**

272 We generated two pools of CSF reference standards as QCs based on biomarker status (AT-  
273 and AT+). These QCs were processed and analyzed (at the beginning, end, and after every 20  
274 samples per plate) identically to the individual clinical samples for testing assay reproducibility.  
275 We analyzed 30 QCs (15 AT- and 15 AT+) over approximately 5 days during the run of clinical  
276 samples. We identified 62 peptides from 51 proteins as reliably measured in the pooled  
277 reference standards. Notably, only 5 of these peptides overlap with previous published PRM  
278 dataset given the unique differences in sample preparation, MS platform and peptide  
279 selection<sup>21</sup>. We included 58 peptides from 51 proteins in our biomarker analysis, plus peptides  
280 specific for the four APOE alleles for proteogenomic confirmation of APOE genotypes<sup>27,28</sup>. The  
281 technical coefficient of variation (CV) of each peptide was calculated based on the peptide  
282 area ratio for the biomarker negative (AT-) and positive (AT+) QCs. We defined CSF peptide  
283 biomarkers with CVs  $\leq 20\%$  as quantified with high precision in these technical replicates which  
284 were un-depleted and unfractionated CSF sample pools. Technical and process reproducibility  
285 for all reported peptides was below 20% (CV < 20%) in at least one pooled reference standard.  
286 The average CVs for all peptides in the AT- and AT+ QCs were 13% and 12%, respectively.  
287 **Supplemental Table 1** contains the QC statistics for the biomarker and APOE allele specific  
288 peptides. Levels of HBA and HBB peptides can be used to assess the levels of potential blood  
289 contamination<sup>29</sup> in each of the CSF samples across individual plates (**Supplemental Fig. 1**).  
290 Correction for blood contamination could improve the statistics; however, no correction was  
291 performed for the statistical analyses presented. We used the protein directions of change to  
292 assess accuracy in the QC pools. The volcano plot between peptides measured in the pools  
293 highlights peptide/protein levels that are consistent with previously reported AD biomarkers  
294 (**Supplemental Fig. 2**)<sup>16,21</sup>.

295

### 296 **Monitoring LC-MS/MS instrument performance**

297 The sample reconstitution solution contained Promega 6x5 LC-MS/MS Peptide Reference Mix  
298 (50 fmol/ $\mu\text{L}$ )<sup>30</sup>. The Promega Peptide Reference Mix provides a convenient way to assess LC  
299 column performance and MS instrument parameters, including sensitivity and dynamic range.  
300 The mix consists of 30 peptides; 6 sets of 5 isotopologues of the same peptide sequence,  
301 differing only in the number of stable, heavy-labeled amino acids incorporated into the  
302 sequence using uniform <sup>13</sup>C and <sup>15</sup>N atoms making them chromatographically  
303 indistinguishable. The isotopologues were specifically synthesized to cover a wide range of  
304 hydrophobicities so that dynamic range could be assess across the gradient profile (**Fig. 2A**).  
305 Each isotopologue represents a series of 10-fold dilutions, estimated to be 1 pmole, 100 fmole,  
306 10 fmole, 1 fmole, and 100 amole for each peptide sequence in a 20  $\mu\text{L}$  injection, a range that  
307 would challenge the lowest limits of detection of the method (**Fig. 2B**). We assessed the raw  
308 peak areas in 423 injections over 5 days to determine the label-free CV for each peptide  
309 isotopologue (**Fig. 2B**). The 100-amole level (0.0001x) was not detected (ND) for any of the  
310 peptide sequences. Based on the label-free CV, we determined the lowest limit of detection  
311 for each peptide to be between 1-10 fmole across the gradient profile with a dynamic range

312 spanning 4 orders of magnitude for all peptides except the latest eluting peptide at 13.3  
313 minutes (**Fig. 2C**).

314

#### 315 **Technical replicate variance**

316 Three individual samples were analyzed in duplicate scattered throughout the sample run  
317 sequence to assess technical replicate variance. We graphed the  $\log_2(\text{ratio})$  for each of 58  
318 biomarker peptides in replicate 1 versus replicate 2 for each sample and determined the  
319 Pearson correlation coefficient with associated P value (**Supplemental Fig. 3**). The analysis  
320 showed a near-identical correlation ( $\rho=0.996-0.998$ ;  $p<1e-200$ ) between each of the technical  
321 replicate pairs for the three individual CSF samples, supporting the same high level of method  
322 reproducibility we found using the QC pools.

323

#### 324 **Concordance between a discovery (ssTMT) and replication (SRM) datasets**

325 Since our peptide targets were largely based on multiple ssTMT datasets<sup>16</sup>, we generated a  
326 representative ssTMT peptide level volcano from one of these datasets comprised of 297  
327 individuals (147 control and 150 AD) (**Fig. 3A**). There are 44 of 62 SRM peptides that overlap  
328 with this ssTMT dataset and are highlighted in yellow on the volcano plot (**Fig. 3A**). To establish  
329 peptide concordance, we also compared the direction of change or effect size ( $\log_2$  fold  
330 change) for 40 overlapping peptides, excluding albumin, hemoglobin, and APOE allele specific  
331 peptides. **Fig. 3B** shows significant correlation ( $\text{cor} = 0.91$ ;  $p = 2.8e-15$ ) between SRM and  
332 ssTMT peptide highlighting the accuracy and concordance of measurements across both MS  
333 assays. Thus, despite substantial differences in chromatography (nanoflow versus standard  
334 flow), MS instrumentation (Orbitrap versus triple quadrupole), and protein quantitation  
335 approaches (ssTMT versus SRM), the selected peptides in this assay are highly reproducible  
336 and robust in their direction of change in AD CSF.

337

#### 338 **Usage Notes**

339 This targeted mass spectrometry dataset serves as a valuable resource for a variety of research  
340 endeavors including, but not limited to, the following applications:

##### 341 **Use case 1: Peptide abundance in CSF**

342 This dataset provides a reference for peptide detectability in CSF under relatively high-  
343 throughput conditions, especially if an investigator wants to determine whether their protein  
344 of interest has abundance above the lower limit of detection in CSF under these analytical  
345 conditions. Raw data deposited on Synapse<sup>22</sup> contains transitions for over 200 peptides that  
346 were robustly detected in CSF discovery proteomics<sup>16,21</sup>.

##### 347 **Use case 2: Using APOE allele specific peptides for genotyping**

348 Apolipoprotein E (ApoE) has three major genetic variants (E2, E3, and E4, encoded by the  $\epsilon 2$ ,  
349  $\epsilon 3$  and  $\epsilon 4$  alleles, respectively) that differ by single amino acid substitutions<sup>31</sup>. APOE genotype  
350 is closely related to AD risk<sup>32</sup> with ApoE4 having the highest risk, ApoE2 the lowest risk, and  
351 ApoE3 with intermediate risk<sup>33,34</sup>. Due to the amino acid substitutions in each variant, there  
352 are allele specific peptides that can be targeted by mass spectrometry<sup>27,35</sup>. We monitored  
353 CLAVYQAGAR (APOE2), LGADMEDVVR (APOE4), LGADMEDVCGR (APOE2 or APOE3), and  
354 LAVYQAGAR (APOE3 or APOE4) to confirm the APOE genotype of each CSF sample in a  
355 concurrent SRM-MS method<sup>22</sup>. The CV for each APOE peptide in each QC is listed in  
356 **Supplemental Table 1**. Previous studies report the association of APOE genotype with various  
357 clinical, neuroimaging, and biomarker measures<sup>36-39</sup>. Exploring the relationship between APOE  
358 status and the CSF biomarker peptides presented requires further analysis reserved for future  
359 studies.

##### 360 **Use case 3: Stage-specific differences in peptide and protein levels**

361 The described cohort includes control, AsymAD, and AD groups across the  
362 Amyloid/Tau/Neurodegeneration (AT/N) framework<sup>40</sup>, which allows for the comparison of  
363 peptide and protein differential abundance across stages of disease. Investigators can focus  
364 on comparisons that are specific to symptomatic AD or those with potential for staging AD by  
365 using the AsymAD group compared to the control group. By comparing candidate biomarkers  
366 using ANOVA (excluding APOE allele specific peptides), we found 41 differentially expressed  
367 peptides (36 proteins) in AsymAD vs controls (**Fig. 4A**), 35 differentially expressed peptides (30  
368 proteins) in AD versus controls (**Fig. 4B**), and 21 differentially expressed peptides (18 proteins)  
369 in AD vs AsymAD (**Fig. 4C**). The Venn diagram summarizes the differentially expressed peptides  
370 across groups in **Fig. 4D**.

371 Using a differential abundance analysis, we were able to stratify the changing proteins as early  
372 or progressive biomarkers of AD (**Fig. 4 and 5**). The log<sub>2</sub>-fold change (Log<sub>2</sub> FC) from the volcano  
373 plots in **Fig. 4** are represented as a heatmap in **Fig. 5A** to illustrate how each peptide is  
374 changing across each group comparison. Twenty-two peptides (21 proteins) were early  
375 biomarkers of AD because they were significantly different in AsymAD versus controls, but not  
376 significantly different in AD versus AsymAD (**Fig. 5A**). A plurality of these proteins mapped to  
377 metabolic enzymes linked to glucose metabolism (PKM, MDH1, ENO1, ALDOA, ENO2, LDHB,  
378 and TPI1, also in **Supplemental Table 2**)<sup>13,14</sup>. SMOC1 and SPP1, markers linked to glial biology  
379 and inflammation<sup>14,16</sup>, were also increased in AsymAD samples compared to controls (**Fig. 5B**,  
380 *top row*). GAPDH, YWHAB and YWHAZ proteins were found to be progressive biomarkers of  
381 AD because the proteins were differentially expressed from Control to AsymAD and from  
382 AsymAD to AD with a consistent trend in direction of change (**Fig. 5B**, *middle row*). Proteins  
383 associated with neuronal/synaptic markers including VGF, NPTX2, NPTXR, and L1CAM were  
384 increased in AsymAD compared to controls but decreased in AD vs controls (**Fig. 5B**, *lower*  
385 *row*). Interestingly, we found 14 peptides (13 proteins) that were up in AsymAD as compared  
386 to Control but down in AD when compared to AsymAD. A majority of these proteins map to  
387 neuronal/synaptic markers including VGF, NPTX2, NPTXR, which are some of the most  
388 correlated proteins in post-mortem brain to an individual's slope of cognitive trajectory in life  
389 (**Fig. 5A and 5B**, *lower row*)<sup>41</sup>.

#### 390 **Use case 4: Correlation of peptide biomarker abundance to Aβ(1-42), Tau, pTau and** 391 **cognitive measures**

392 The comparison of existing biomarkers to the SRM peptide measurements can be  
393 accomplished by correlation, where the degree of correlation indicates how similar a peptide  
394 measurement is to the established immunoassay-measured biomarkers of Aβ(1-42), total Tau,  
395 and pTau as well as cognition (MoCA score). In **Fig. 6A**, we demonstrate that 57 of the 58  
396 biomarker peptides have significant correlation to at least one of the above biomarkers, or the  
397 ratio of total Tau/Aβ. Individual correlation scatterplots and linear fit lines for three of the  
398 peptides (SMOC1: AQALEQAK, YWHAZ: VVSSIEQK, and VGF: EPVAGDAVPGPK) are provided in  
399 **Fig. 6B**. Significant correlations of these peptides to the established biomarker and cognitive  
400 measures indicate the potential of these measurements to classify or stage disease  
401 progression. The targeted SRM measurement correlations largely agree with those observed  
402 from unbiased discovery proteomics<sup>42</sup> and parallel reaction monitoring<sup>21</sup> experiments.

#### 403 **Use case 5: Receiver-operating characteristic (ROC) analysis for evaluating biomarker** 404 **diagnostic capability**

405 The capacity for peptide measurements to serve as a diagnostic biomarker distinguishing  
406 individuals with AD and even asymptomatic disease from individuals not on a trajectory to  
407 develop AD is well-established, with secreted amyloid and tau peptide measurements in CSF  
408 being the current gold standard for interrogation of patients' AD stage from their CSF<sup>43</sup> where  
409 CSF Aβ(1-42) concentration inversely correlates to plaque deposition in the living brain<sup>44</sup>. The  
410 measurements of additional peptides collected here are appropriate for comparison to

411 immunoassay measurements of CSF amyloid and Tau biomarker positivity, or a dichotomized  
412 cognition rating, or other ancillary traits such as diagnosis for the 390 individuals. To  
413 demonstrate this utility, we performed receiver-operating characteristic (ROC) curve analysis  
414 and calculated the area under the curve (AUC) for all 62 peptide measures as fitting a logistic  
415 regression to 3 subsets of samples divided to represent known pairs of disease stages, namely  
416 AD versus control, AsymAD versus control, and AD vs AsymAD (**Fig. 7** and **Supplemental Table**  
417 **4**). The top performing peptide for the YWHAZ gene product 14-3-3  $\zeta$  protein demonstrated  
418 an AUC of 89.5% discrimination of AD from control cases consistent with previous  
419 studies<sup>21,45,46</sup>. SMOC1 AUC of 81.8% was the best performing peptide for discrimination of  
420 AsymAD from control groups. In contrast, the synaptic peptides to NPTX2 (AUC of 74.0%),  
421 NPTXR (AUC of 71.1%), VGF (AUC of 70.1%) and SCG2 (AUC of 69.8%) best discriminated AD  
422 from AsymAD groups suggesting that neurodegeneration due to AD pathology is occurring in  
423 the symptomatic phase of disease<sup>47</sup>. **Fig. 7** shows the top five peptides by AUC for each of the  
424 three comparisons, highlighting the potential of this data set to aid in the design or validation  
425 of stage-specific biomarkers. Additional future analysis using these peptides alone or in  
426 combination could be used to subtype, predict disease onset, and gauge treatment efficacy.

## 427 **Code Availability**

428 Custom code generating use case figures and tables including correlation plots, volcanoes,  
429 Venn diagram, annotated heatmap, statistics tables, and ROC curves is available for download  
430 with registration for a free account on synapse.org. The code is available as R scripts from  
431 <https://doi.org/10.7303/syn35927166> (the Analysis folder) deposited on Synapse<sup>22</sup>. These  
432 scripts were run as provided on R version 4.0.2 with the two provided input files to generate  
433 outputs.

## 434 **Acknowledgements**

435 This study was supported by the following National Institutes of Health funding mechanisms:  
436 U01AG061357 (A.I.L and N.T.S), R01AG070937-01 (J.J.L) and P30AG066511 (A.I.L). We  
437 acknowledge our colleagues at Emory for providing critical feedback.

## 438 **Author contributions**

439 Conceptualization, C.M.W., L.P., D.M.D., J.J.L., A.I.L., B.R.R, N.T.S.; Methodology, C.M.W.,  
440 E.B.D, L.P., D.M.D., E.M., E.K.C., B.R.R, N.T.S.; Investigation and Formal Analysis, C.M.W., E.B.D,  
441 L.P., D.M.D., B.R.R, N.T.S.; Writing – Original Draft, C.M.W., E.B.D., N.T.S.; Writing – Review  
442 and Editing, C.M.W., E.C.B.J, B.R.R., J.J.L., A.I.L., N.T.S.; Funding Acquisition, A.I.L. and N.T.S.;

## 443 **Competing interests**

444 The authors declare no competing interests.

## 445 **Figure Legends**

446 **Figure 1. Cohort characteristics.** A total of 390 samples (133 controls, 127 AsymAD, 130 AD  
447 unless otherwise noted) were analyzed using the following characteristics for grouping. **(A)**  
448 Age range across each group of the cohort was carefully selected to balance for age and sex  
449 (**Supplemental Table 1**). **(B)** Cognition was assessed using the Montreal Cognitive Assessment  
450 (MoCA) score; there is no significant difference in scores between the Control and AsymAD  
451 groups serving as the two cognitively normal diagnostic groups (133 controls, 127 AsymAD,  
452 124 AD). The Roche Diagnostics Elecsys® platform was used for CSF biomarker measurements  
453 for A $\beta$ (1-42) **(C)**, Total Tau (133 controls, 127 AsymAD, 129 AD) **(D)**, and pTau **(E)** (pg/mL)  
454 showing the significance between groups for each measurement. **(F)** Tau/A $\beta$  ratio data across



461 control, AsymAD and AD groups. There was no significant difference between AsymAD and AD  
462 groups to serve as our biomarker positive groups (133 controls, 127 AsymAD, 129 AD). The  
463 significance of the pairwise comparisons is indicated by overlain annotation of 'ns' (not  
464 significant;  $p>0.05$ ) or asterisks; \*\*\*\* $p\leq 0.0001$ .

465

466 **Figure 2. Isotopologue peptide internal reference standards to determine consistency of LC-**  
467 **MS/MS platform.** Each of the CSF samples were spiked with a six-peptide, 5 isotopologue  
468 concentration LC-MS/MS Peptide Reference Mix from Promega (50 fmol/ $\mu$ L). (A) Extracted ion  
469 chromatogram for the 6 peptide (1pmol) mixture illustrating the wide range of retention times  
470 due to their hydrophobicity. (B) The raw peak areas in 423 injections over 5 days were used to  
471 determine the label-free CV for each peptide isotopologue estimating the lowest limits of  
472 detection to be between 1-10 fmole for each peptide. (C) The 5 unique isotopologues are used  
473 to assess the dynamic range across the gradient profile and each peptide demonstrates  
474 linearity across 3-4 orders of magnitude in the batch of 423 injections. Error bars represent  
475 the standard deviation across 423 injections.

476 **Figure 3. Peptide concordance between SRM and ssTMT datasets.** (A) Volcano plot displaying  
477 the  $\log_2$  fold change (FC) (x-axis) against t-test  $\log_{10}$  p-value (y-axis) for all peptides ( $n=2,340$ )  
478 comparing AD ( $n=150$ ) versus Controls ( $n=147$ ). Cutoffs were determined by significant  
479 differential expression ( $p<0.05$ ) between control and AD cases. Peptides with significantly  
480 decreased levels in AD are shown in blue while peptides with significantly increased levels in  
481 disease were indicated in red. 44 of 62 SRM peptides that overlap with this ssTMT dataset and  
482 SRM are highlighted as larger yellow points with black text labels. Red text and traces to red  
483 points are labels for peptides not included in the current SRM study that were significantly  
484 upregulated in the ssTMT dataset. (B) Correlation between the fold-change (AD vs control) of  
485 all selected overlapping peptides ( $n=40$ ) across SRM (x-axis) and ssTMT (y-axis) were strongly  
486 correlated ( $\text{cor}=0.91$ ,  $p=2.8e-15$ ).

487

488 **Figure 4. Differential expression analysis across stages of AD.** ANOVA analysis with Tukey *post*  
489 *hoc* FDR was performed for pairwise comparison of mean  $\log_2(\text{ratio})$  differences between the  
490 3 stages of AD (i.e., Control, AsymAD and AD) of  $N=390$  total case samples and plotted as a  
491 volcano. Significance threshold for counting of peptides was  $p < 0.05$  (dashed horizontal line).  
492 Differentially expressed peptides for (A) AsymAD ( $N=127$ ) versus control ( $N=133$ ), (B) AD  
493 ( $N=130$ ) versus control, and (C) AD versus AsymAD are labeled by their gene symbols. (D)  
494 Counts of peptides with significant difference in any of the 3 dichotomous comparisons are  
495 presented as a Venn diagram. Full statistics from the ANOVA and Tukey post-hoc analysis is  
496 presented in **Supplemental Table 2**.

497

498 **Figure 5. Stratifying early from progressive biomarkers of AD.** (A) The magnitude of positive  
499 (red) and negative (blue) changes are shown on a gradient color scale heatmap representing  
500 mean  $\log_2$ -fold change ( $\text{Log}_2\text{FC}$ ) for each of 49 peptides significant in any of the 3 group  
501 comparisons. Tukey significance of the pairwise comparisons is indicated by overlain asterisks;  
502 \* $p<0.05$ , \*\* $p<0.01$ , \*\*\* $p<0.001$ . (B) Peptide abundance levels of selected panel markers that  
503 are differentially expressed between groups. The upper row highlights biomarkers that are  
504 significantly different in AsymAD versus controls, but not significantly different in AsymAD  
505 versus AD. The middle row of 3 peptides highlights progressive biomarkers of AD, which show  
506 a stepwise increase in abundance from control to AsymAD to AD cases. The bottom row  
507 highlights a set of proteins that are increased in AsymAD compared to controls but decreased  
508 in AD versus control or AsymAD samples.

509

510 **Figure 6. Correlating CSF peptide biomarker abundances to amyloid, Tau, and cognitive**  
511 **measures.** (A) Positive (red) and negative (blue) Pearson correlations between biomarker  
512 peptide abundance and immunoassay measures of A $\beta$ (1-42), total Tau, phospho-T181 Tau  
513 (pTau), ratio of total Tau/A $\beta$  and cognition (MoCA score). Student's *t* test significance is  
514 indicated by overlain asterisks; \* $p < 0.05$ , \*\* $p < 0.01$ , \*\*\* $p < 0.001$ . (B) Individual correlation  
515 scatterplots are shown for SMOC1 (upper row), YWHAZ (middle row), and VGF (lower row).  
516 Individual cases are colored by their diagnosis; blue for controls, red for AsymAD cases, and  
517 green for AD cases. Amyloid immunoassay measures of 1,700 (maximum, saturated value in  
518 the assay) were not considered for correlation.

519  
520 **Figure 7. Receiver-operating characteristic (ROC) curve analysis of peptide diagnostic**  
521 **potential.** ROC curves for each of three pairs of diagnosed case groups were generated to  
522 determine the top-ranked diagnostic biomarker peptides among the 58-peptide panel plus 4  
523 APOE specific peptides. (A) A total of 263 AD (N=130) and control (N=133) CSF case samples  
524 were classified according to the logistic fit for each peptide's  $\log_2$ (ratio) measurements across  
525 these samples, and the top 5 ranked by AUC are shown. (B) Top five performing peptides for  
526 discerning AsymAD (N=127) from control (N=133) case diagnosis groups are provided with  
527 AUCs, nominating these peptides as potential markers of pre-symptomatic disease, and as  
528 cognates for AT+ biomarker positivity. (C) Symptomatic AD (N=130) and AsymAD (N=127)  
529 discerning peptides were ranked by AUC and the top five ROC curves are shown and  
530 nominated as cognate CSF measures for compromised patient cognition.

531

## 532 **Supplemental Data**

533

534 **Supplemental Figure 1. Monitoring background peptide levels in CSF.** Three proteins were  
535 monitored for levels of potential blood contamination in each of the CSF samples. The peptide  
536 ratio for hemoglobin subunit alpha (A), hemoglobin subunit beta (B), and albumin (C and D)  
537 peptides are plotted for each of the CSF samples (N=423) in acquisition order.

538

539 **Supplemental Figure 2. Differentially abundant peptides representing changed proteins in**  
540 **AT- vs AT+ QC CSF pools.** The differentially abundant proteins in the QC pools were used to  
541 check the accuracy of the fold change consistent with our other studies<sup>16</sup>. We found 21  
542 upregulated and 10 downregulated peptides. This result validated the direction of change of  
543 six proteins nominally significantly downregulated in previously published discovery  
544 proteomics (PON1, APOC1, NPTX2, VGF, NPTXR, and SCG2), and of sixteen proteins previously  
545 reported as upregulated (YWHAZ, GDA, CHI3L1, PKM, CALM2, SMOC1, YWHAB, MDH1,  
546 ALDOA, ENO1, GOT1, PPIA, DDAH1, PEBP1, PARK7, and SPP1)<sup>16,21</sup>.

547

548 **Supplemental Figure 3. Technical reproducibility of peptide measurements in replicate CSF**  
549 **samples.** Pearson correlation and p-value of replicate measures of 58 peptides in the 3  
550 replicated CSF samples that were analyzed randomly within the series of 423 injections by  
551 SRM-MS.

552

553 **Supplemental Table 1.** Coefficient of variation (CV) values for 58 biomarker peptides and APOE  
554 allele specific peptides in AT- and AT+ QC pools.

555

556 **Supplemental Table 2.** ANOVA of differential abundance analysis for 58 biomarker peptides  
557 across Control, AsymAD and AD sample pairwise group comparisons. The SRM proteins were  
558 also cross-referenced with protein data and module membership from Johnson et al.  
559 Consensus Network<sup>48</sup>, and mapped to CSF protein panels from Higginbotham et al. Integrated  
560 Proteomic analysis<sup>16</sup>.

561

562 **Supplemental Table 3.** Pearson correlations ( $\rho$ ), Student p values of correlation significance,  
563 and numbers of paired observations for correlation of biomarker peptide abundances to  
564 immunoassay measures of A $\beta$ (1-42), total Tau, phospho-T181 Tau, and the ratio of total Tau/  
565 A $\beta$ .

566  
567 **Supplemental Table 4.** ROC curve statistics including AUC, p, 95% DeLong confidence interval,  
568 accuracy, specificity, and sensitivity for dichotomous diagnosis case sample groups.

## 569 570 **References**

- 571  
572 1 Scheltens, P. *et al.* Alzheimer's disease. *The Lancet* **397**, 1577-1590,  
573 doi:10.1016/S0140-6736(20)32205-4 (2021).
- 574 2 Duyckaerts, C., Delatour, B. & Potier, M.-C. Classification and basic pathology of  
575 Alzheimer disease. *Acta neuropathologica* **118**, 5-36 (2009).
- 576 3 Jack Jr, C. R. *et al.* NIA-AA research framework: toward a biological definition of  
577 Alzheimer's disease. *Alzheimer's & Dementia* **14**, 535-562 (2018).
- 578 4 Mattsson-Carlgen, N. *et al.* Cerebrospinal fluid biomarkers in autopsy-confirmed  
579 Alzheimer disease and frontotemporal lobar degeneration. *Neurology* **98**, e1137-  
580 e1150 (2022).
- 581 5 Zetterberg, H. & Blennow, K. Moving fluid biomarkers for Alzheimer's disease from  
582 research tools to routine clinical diagnostics. *Molecular neurodegeneration* **16**, 1-7  
583 (2021).
- 584 6 Long, J. M. & Holtzman, D. M. Alzheimer disease: an update on pathobiology and  
585 treatment strategies. *Cell* **179**, 312-339 (2019).
- 586 7 Rayaprolu, S. *et al.* Systems-based proteomics to resolve the biology of Alzheimer's  
587 disease beyond amyloid and tau. *Neuropsychopharmacology* **46**, 98-115 (2021).
- 588 8 Sperling, R. A. *et al.* Toward defining the preclinical stages of Alzheimer's disease:  
589 Recommendations from the National Institute on Aging-Alzheimer's Association  
590 workgroups on diagnostic guidelines for Alzheimer's disease. *Alzheimer's & dementia*  
591 **7**, 280-292 (2011).
- 592 9 Dubois, B. *et al.* Preclinical Alzheimer's disease: definition, natural history, and  
593 diagnostic criteria. *Alzheimer's & Dementia* **12**, 292-323 (2016).
- 594 10 Hasin, Y., Seldin, M. & Lusis, A. Multi-omics approaches to disease. *Genome biology*  
595 **18**, 1-15 (2017).
- 596 11 Seyfried, N. T. *et al.* A Multi-network Approach Identifies Protein-Specific Co-  
597 expression in Asymptomatic and Symptomatic Alzheimer's Disease. *Cell Syst* **4**, 60-72  
598 e64, doi:10.1016/j.cels.2016.11.006 (2017).
- 599 12 Johnson, E. C. B. *et al.* Deep proteomic network analysis of Alzheimer's disease brain  
600 reveals alterations in RNA binding proteins and RNA splicing associated with disease.  
601 *Mol Neurodegener* **13**, 52, doi:10.1186/s13024-018-0282-4 (2018).
- 602 13 Johnson, E. C. B. *et al.* A Consensus Proteomic Analysis of Alzheimer's Disease Brain  
603 and Cerebrospinal Fluid Reveals Early Changes in Energy Metabolism Associated with  
604 Microglia and Astrocyte Activation. *bioRxiv*, 802959, doi:10.1101/802959 (2019).
- 605 14 Johnson, E. C. *et al.* Large-scale proteomic analysis of Alzheimer's disease brain and  
606 cerebrospinal fluid reveals early changes in energy metabolism associated with  
607 microglia and astrocyte activation. *Nature medicine* **26**, 769-780 (2020).
- 608 15 Blennow, K. & Zetterberg, H. Biomarkers for Alzheimer's disease: current status and  
609 prospects for the future. *Journal of internal medicine* **284**, 643-663 (2018).
- 610 16 Higginbotham, L. *et al.* Integrated proteomics reveals brain-based cerebrospinal fluid  
611 biomarkers in asymptomatic and symptomatic Alzheimer's disease. *Science advances*  
612 **6**, eaaz9360 (2020).

- 613 17 Picotti, P. & Aebersold, R. Selected reaction monitoring–based proteomics: workflows,  
614 potential, pitfalls and future directions. *Nature methods* **9**, 555-566 (2012).
- 615 18 Bittner, T. *et al.* Technical performance of a novel, fully automated  
616 electrochemiluminescence immunoassay for the quantitation of beta-amyloid (1-42)  
617 in human cerebrospinal fluid. *Alzheimers Dement* **12**, 517-526,  
618 doi:10.1016/j.jalz.2015.09.009 (2016).
- 619 19 Hansson, O. *et al.* CSF biomarkers of Alzheimer's disease concord with amyloid-beta  
620 PET and predict clinical progression: A study of fully automated immunoassays in  
621 BioFINDER and ADNI cohorts. *Alzheimers Dement* **14**, 1470-1481,  
622 doi:10.1016/j.jalz.2018.01.010 (2018).
- 623 20 Schindler, S. E. *et al.* Cerebrospinal fluid biomarkers measured by Elecsys assays  
624 compared to amyloid imaging. *Alzheimers Dement*, doi:10.1016/j.jalz.2018.01.013  
625 (2018).
- 626 21 Zhou, M. *et al.* Targeted mass spectrometry to quantify brain-derived cerebrospinal  
627 fluid biomarkers in Alzheimer's disease. *Clinical Proteomics* **17**, 1-14 (2020).
- 628 22 Watson, C. M., Dammer, E.B., and Seyfried, N.T. Emory AD CSF SRM. *Synapse*,  
629 doi:<https://doi.org/10.7303/syn34054965> (2022).
- 630 23 MacLean, B. *et al.* Skyline: an open source document editor for creating and analyzing  
631 targeted proteomics experiments. *Bioinformatics* **26**, 966-968 (2010).
- 632 24 Pino, L. K. *et al.* The Skyline ecosystem: Informatics for quantitative mass spectrometry  
633 proteomics. *Mass spectrometry reviews* **39**, 229-244 (2020).
- 634 25 MacLean, B. *et al.* Effect of collision energy optimization on the measurement of  
635 peptides by selected reaction monitoring (SRM) mass spectrometry. *Analytical*  
636 *chemistry* **82**, 10116-10124 (2010).
- 637 26 Kulak, N. A., Pichler, G., Paron, I., Nagaraj, N. & Mann, M. Minimal, encapsulated  
638 proteomic-sample processing applied to copy-number estimation in eukaryotic cells.  
639 *Nature methods* **11**, 319-324 (2014).
- 640 27 Simon, R. *et al.* Total ApoE and ApoE4 isoform assays in an Alzheimer's disease case-  
641 control study by targeted mass spectrometry (n= 669): a pilot assay for methionine-  
642 containing proteotypic peptides. *Molecular & Cellular Proteomics* **11**, 1389-1403  
643 (2012).
- 644 28 Rezeli, M. *et al.* Quantification of total apolipoprotein E and its specific isoforms in  
645 cerebrospinal fluid and blood in Alzheimer's disease and other neurodegenerative  
646 diseases. *EuPA Open Proteomics* **8**, 137-143 (2015).
- 647 29 Geyer, P. E. *et al.* Plasma Proteome Profiling to detect and avoid sample-related biases  
648 in biomarker studies. *EMBO molecular medicine* **11**, e10427 (2019).
- 649 30 Beri, J., Rosenblatt, M. M., Strauss, E., Urh, M. & Bereman, M. S. Reagent for evaluating  
650 liquid chromatography–tandem mass spectrometry (LC-MS/MS) performance in  
651 bottom-up proteomic experiments. *Analytical chemistry* **87**, 11635-11640 (2015).
- 652 31 Hatters, D. M., Peters-Libeu, C. A. & Weisgraber, K. H. Apolipoprotein E structure:  
653 insights into function. *Trends in biochemical sciences* **31**, 445-454 (2006).
- 654 32 Saunders, A. M. *et al.* Association of apolipoprotein E allele  $\epsilon$ 4 with late-onset familial  
655 and sporadic Alzheimer's disease. *Neurology* **43**, 1467-1467 (1993).
- 656 33 Farrer, L. A. *et al.* Effects of age, sex, and ethnicity on the association between  
657 apolipoprotein E genotype and Alzheimer disease. A meta-analysis. APOE and  
658 Alzheimer Disease Meta Analysis Consortium. *JAMA* **278**, 1349-1356 (1997).
- 659 34 Heffernan, A. L., Chidgey, C., Peng, P., Masters, C. L. & Roberts, B. R. The neurobiology  
660 and age-related prevalence of the  $\epsilon$ 4 allele of apolipoprotein E in Alzheimer's disease  
661 cohorts. *Journal of Molecular Neuroscience* **60**, 316-324 (2016).
- 662 35 Minta, K. *et al.* Quantification of total apolipoprotein E and its isoforms in  
663 cerebrospinal fluid from patients with neurodegenerative diseases. *Alzheimer's*  
664 *research & therapy* **12**, 1-11 (2020).

- 665 36 Bussy, A. *et al.* Effect of apolipoprotein E4 on clinical, neuroimaging, and biomarker  
666 measures in noncarrier participants in the Dominantly Inherited Alzheimer Network.  
667 *Neurobiology of aging* **75**, 42-50 (2019).
- 668 37 El-Lebedy, D., Raslan, H. M. & Mohammed, A. M. Apolipoprotein E gene polymorphism  
669 and risk of type 2 diabetes and cardiovascular disease. *Cardiovascular diabetology* **15**,  
670 1-11 (2016).
- 671 38 Morris, J. C. *et al.* APOE predicts amyloid-beta but not tau Alzheimer pathology in  
672 cognitively normal aging. *Ann Neurol* **67**, 122-131, doi:10.1002/ana.21843 (2010).
- 673 39 Grimmer, T. *et al.* Progression of cerebral amyloid load is associated with the  
674 apolipoprotein E  $\epsilon$ 4 genotype in Alzheimer's disease. *Biological psychiatry* **68**, 879-884  
675 (2010).
- 676 40 Knopman, D. S. *et al.* The National Institute on Aging and the Alzheimer's Association  
677 research framework for Alzheimer's disease: perspectives from the research  
678 roundtable. *Alzheimer's & Dementia* **14**, 563-575 (2018).
- 679 41 Wingo, A. P. *et al.* Large-scale proteomic analysis of human brain identifies proteins  
680 associated with cognitive trajectory in advanced age. *Nature communications* **10**, 1-  
681 14 (2019).
- 682 42 Dammer, E. B. *et al.* Multi-Platform Proteomic Analysis of Alzheimer's Disease  
683 Cerebrospinal Fluid and Plasma Reveals Network Biomarkers Associated with  
684 Proteostasis and the Matrisome. *bioRxiv* (2022).
- 685 43 Bertens, D., Knol, D. L., Scheltens, P. & Visser, P. J. Temporal evolution of biomarkers  
686 and cognitive markers in the asymptomatic, MCI, and dementia stage of Alzheimer's  
687 disease. *Alzheimer's & Dementia* **11**, 511-522,  
688 doi:<https://doi.org/10.1016/j.jalz.2014.05.1754> (2015).
- 689 44 Shokouhi, S. *et al.* Reference tissue normalization in longitudinal 18F-florbetapir  
690 positron emission tomography of late mild cognitive impairment. *Alzheimer's*  
691 *Research & Therapy* **8**, 2, doi:10.1186/s13195-016-0172-3 (2016).
- 692 45 Sathe, G. *et al.* Quantitative proteomic profiling of cerebrospinal fluid to identify  
693 candidate biomarkers for Alzheimer's disease. *PROTEOMICS—Clinical Applications* **13**,  
694 1800105 (2019).
- 695 46 Bader, J. M. *et al.* Proteome profiling in cerebrospinal fluid reveals novel biomarkers  
696 of Alzheimer's disease. *Molecular systems biology* **16**, e9356 (2020).
- 697 47 Libiger, O. *et al.* Longitudinal CSF proteomics identifies NPTX2 as a prognostic  
698 biomarker of Alzheimer's disease. *Alzheimer's & Dementia* **17**, 1976-1987 (2021).
- 699 48 Johnson, E. C. *et al.* Large-scale deep multi-layer analysis of Alzheimer's disease brain  
700 reveals strong proteomic disease-related changes not observed at the RNA level.  
701 *Nature neuroscience* **25**, 213-225 (2022).
- 702



Table 1. Cohort Characteristics

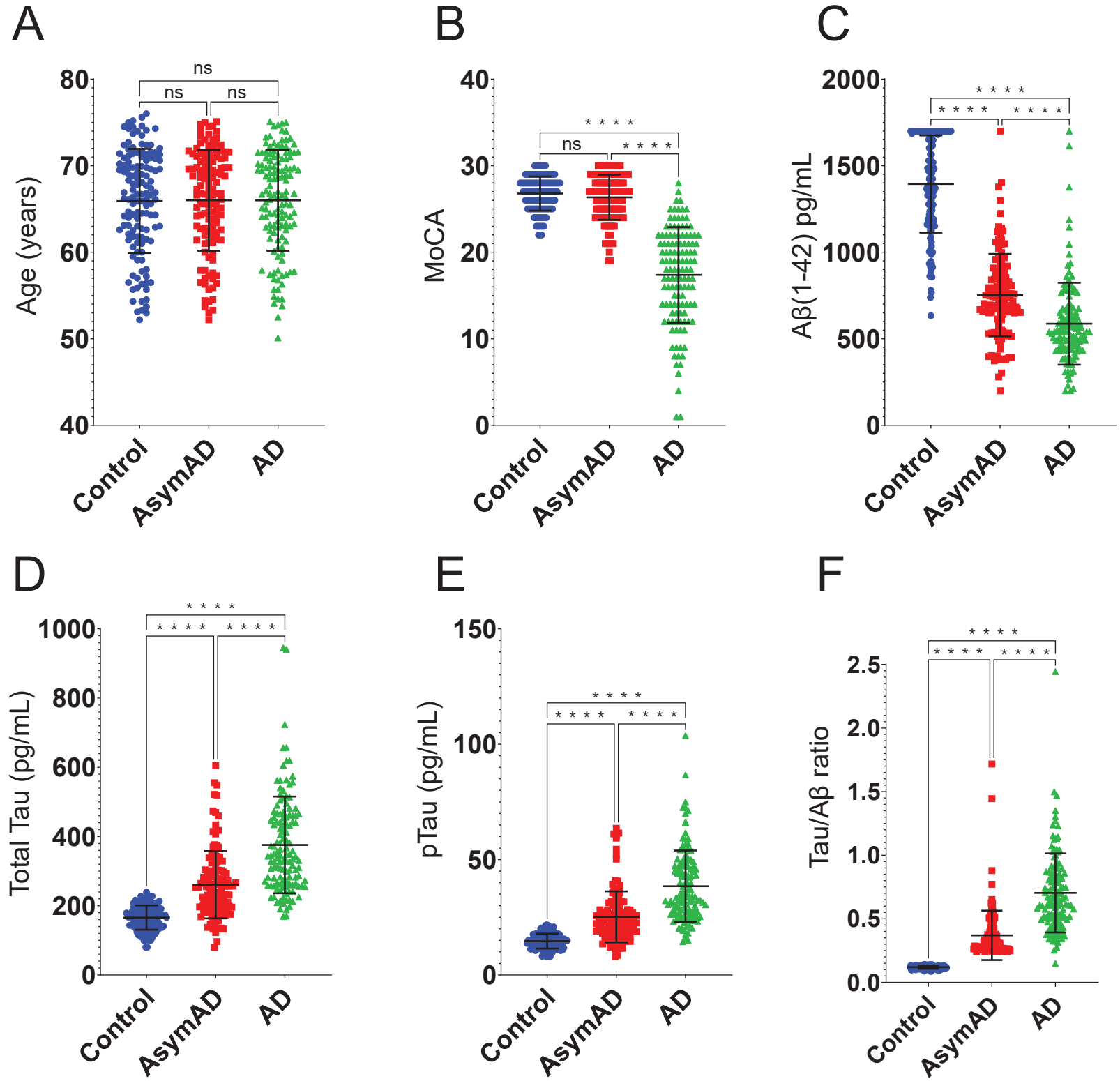
Sample Group	CT	AsymAD	AD
Sample Size	N=133	N=127	N=130
Characteristics			
Sex	99 F, 34 M	94 F, 33 M	97 F, 33 M
Age <sup>a</sup>	66 ± 6	66 ± 6	66 ± 6
MoCA <sup>b</sup>	26.8 ± 2.0	26.4 ± 2.6	17.4 ± 5.5
A $\beta$ <sub>42</sub> <sup>b</sup>	1394.0 ± 280.7	752.0 ± 238.2	587.0 ± 236.8
tTau <sup>b</sup>	165.8 ± 35.0	260.8 ± 97.2	375.7 ± 139.6
pTau <sup>b</sup>	14.7 ± 3.2	25.2 ± 11.1	38.5 ± 15.5

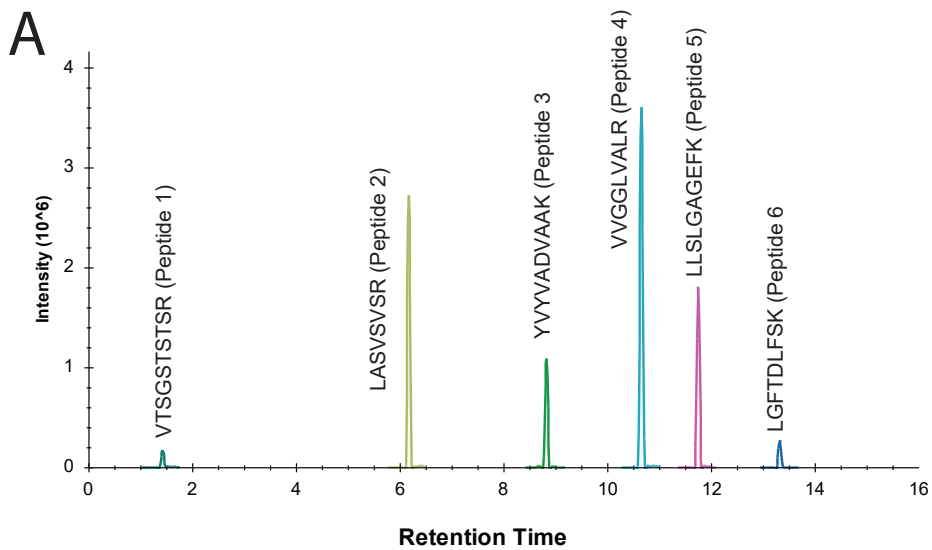
<sup>a</sup> Age in years. Values given as average ± standard deviation

<sup>b</sup> MoCA, A $\beta$ <sub>42</sub>, tTau, and pTau in pg/mL. Values given in average ± standard deviation

Abbreviations: CT, Control; AD, Alzheimer's disease; MoCA, Montreal Cognitive Assessment

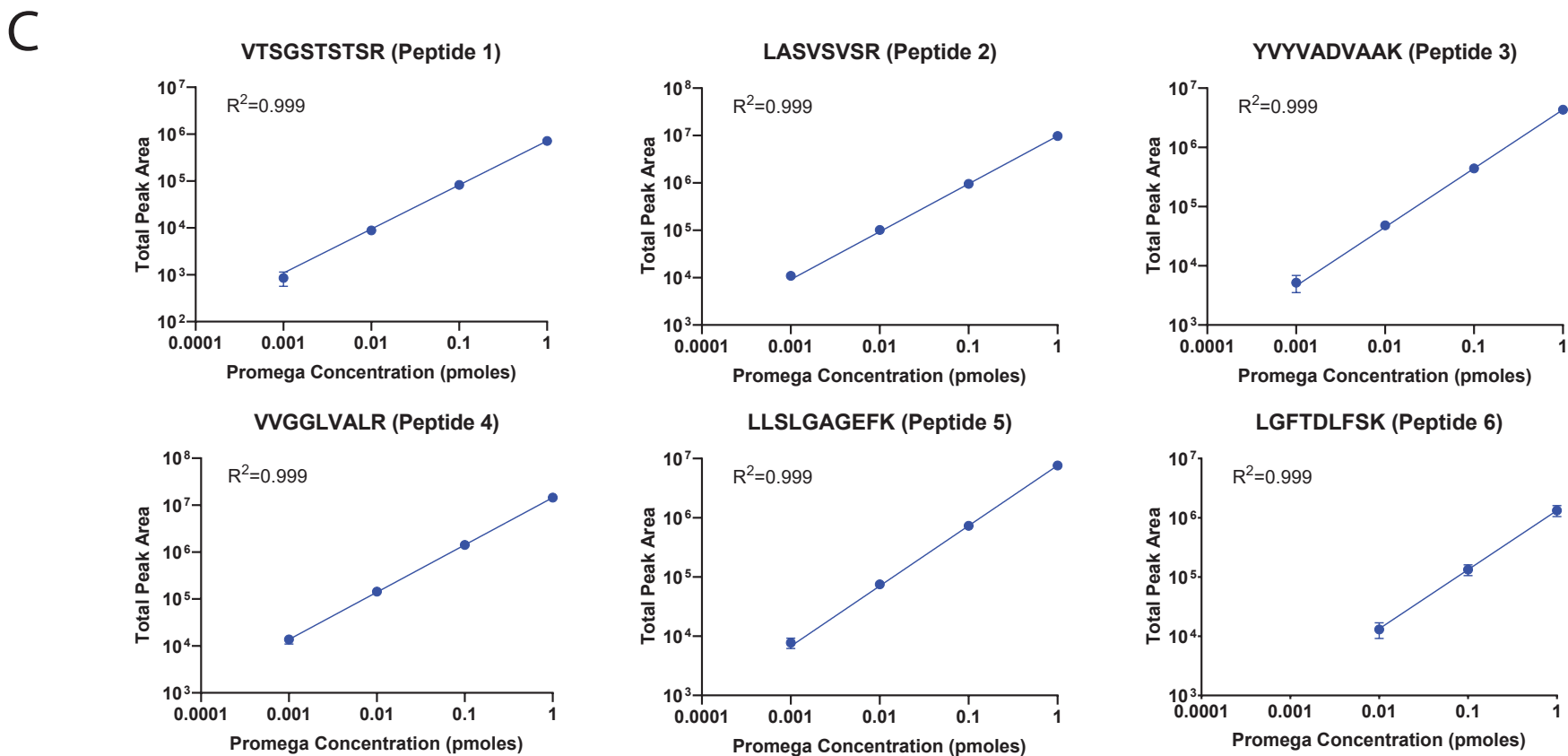
Figure 1



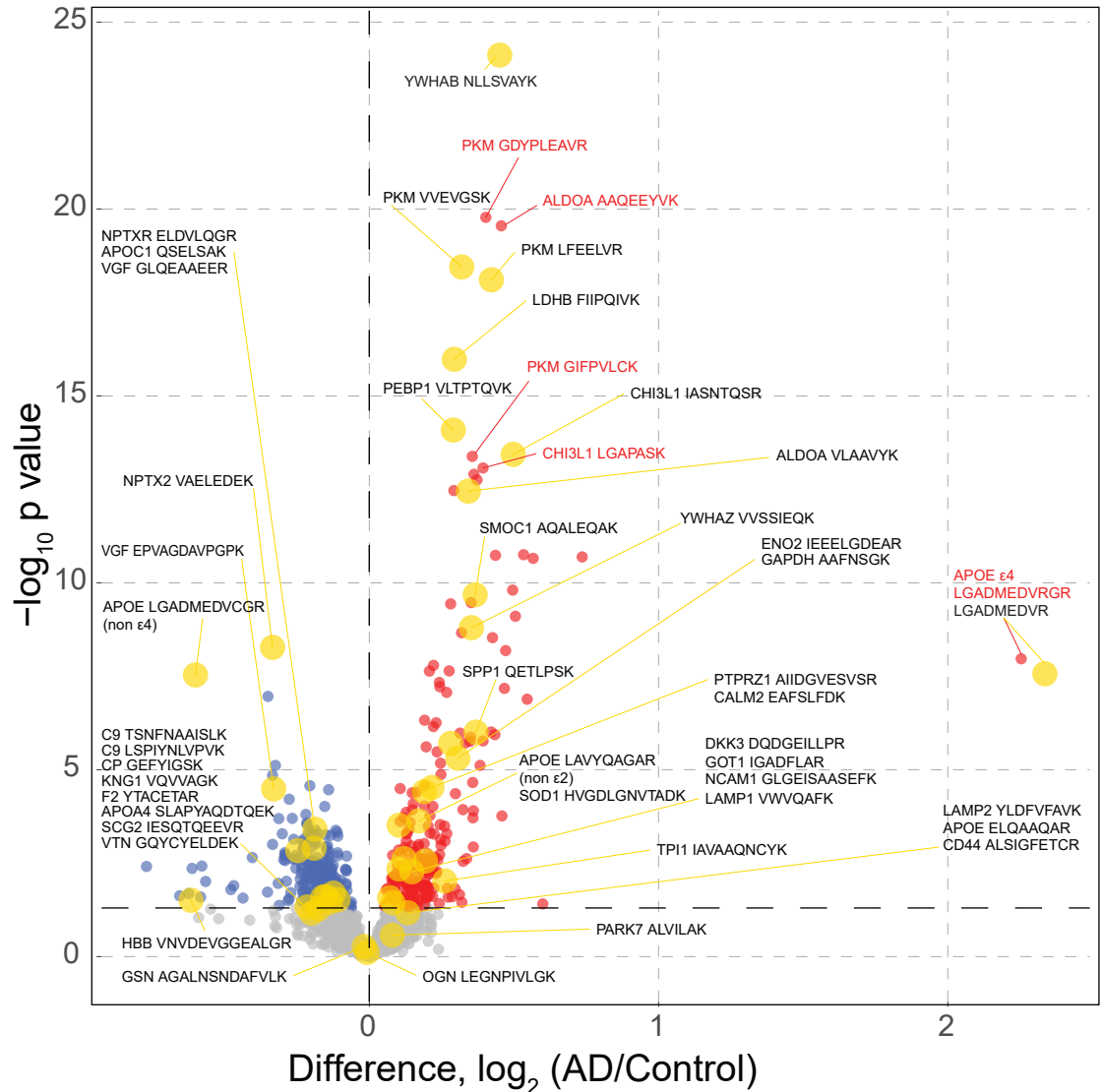


**B**

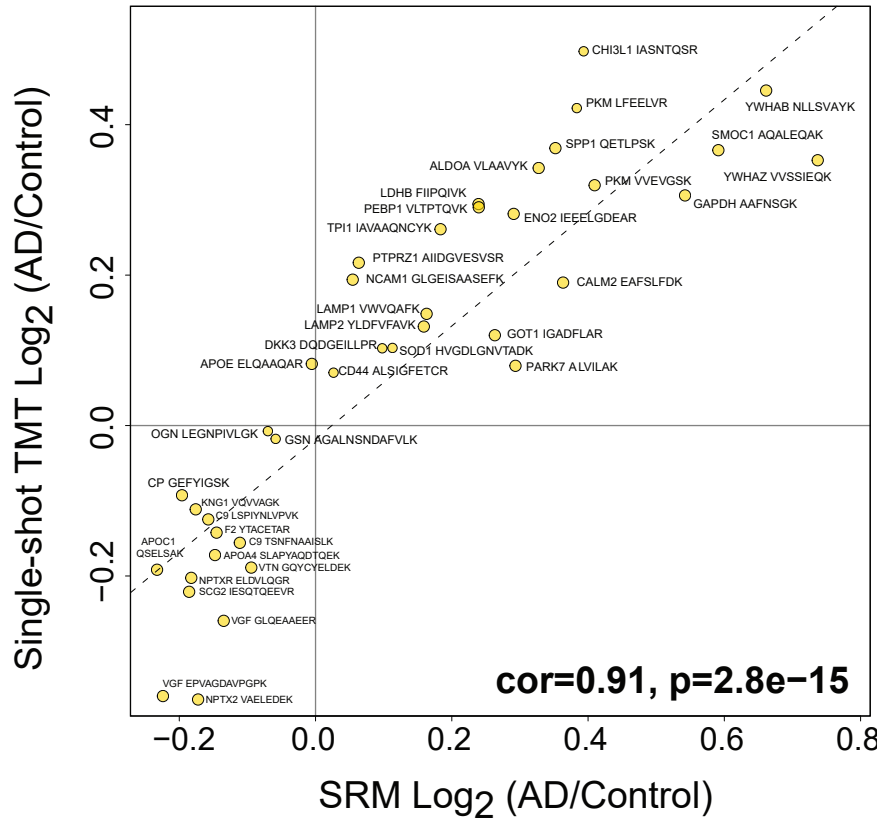
Promega Peptide Sequence	Average Retention Time (min)	1 pmole (1x)	100 fmole (0.1x)	10 fmole (0.01x)	1 fmole (0.001x)	100 amole (0.0001x)
VTSGSTSTR	1.42	17%	17%	18%	34%	ND
LASVSVSR	6.17	7%	8%	8%	17%	ND
YVYVADVAAK	8.83	11%	11%	13%	32%	ND
VVGGLVALR	10.65	8%	8%	9%	20%	ND
LLSLGAGEFK	11.75	9%	9%	10%	20%	ND
LGFTDLFSK	13.33	21%	21%	30%	ND	ND

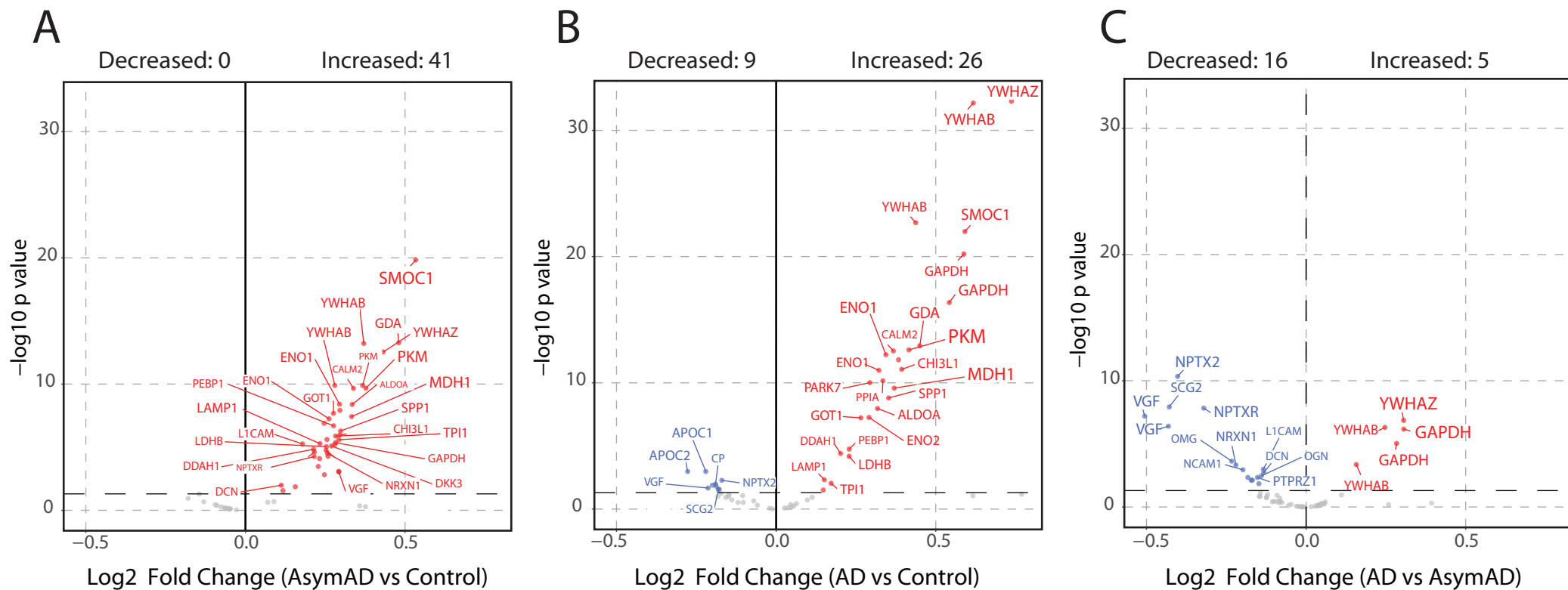


A



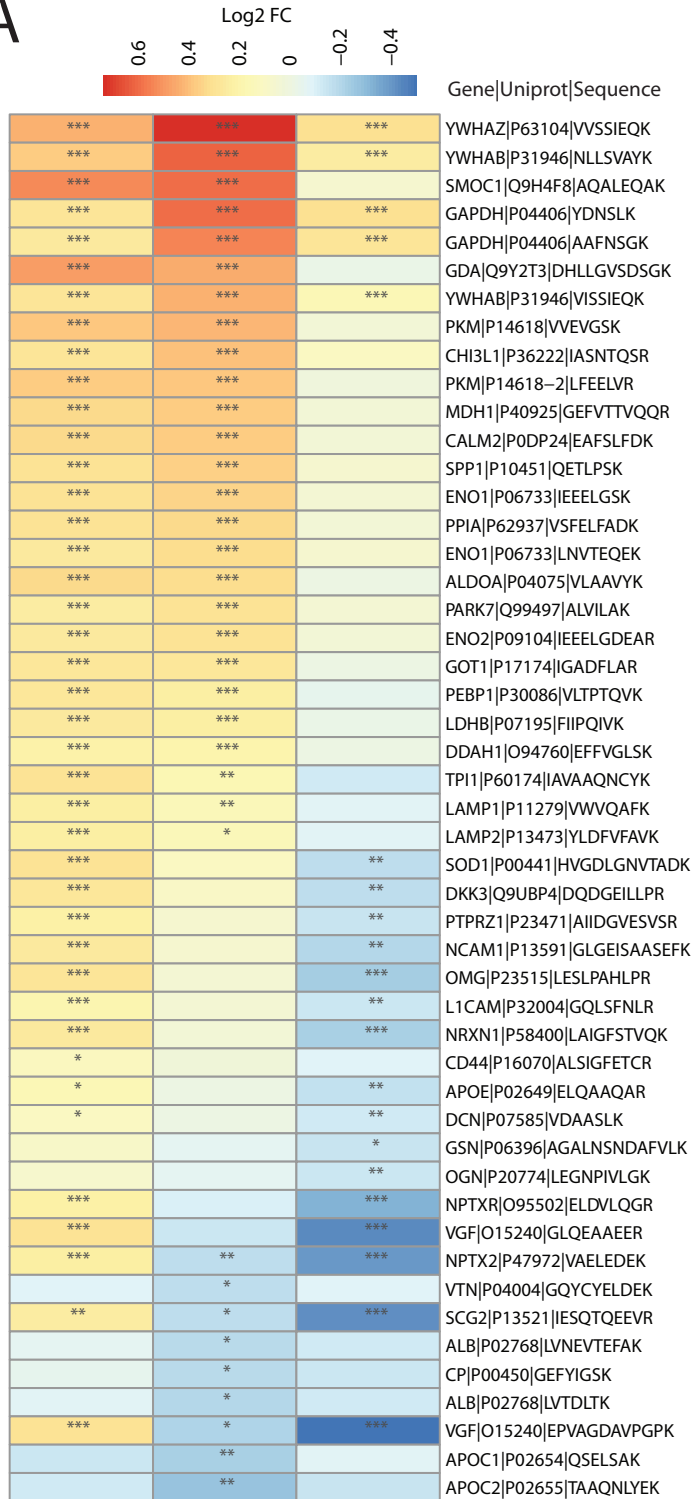
B





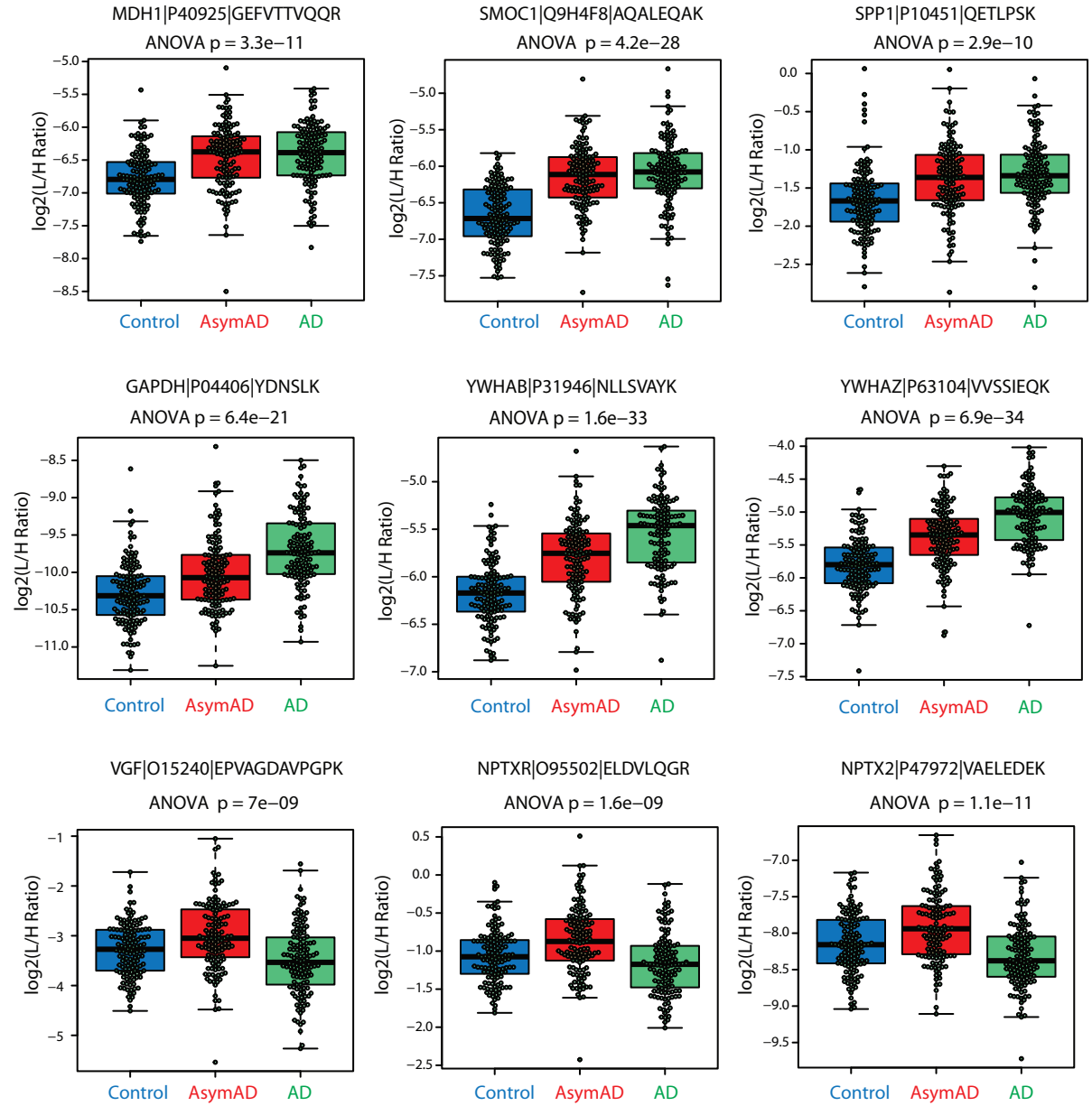


A

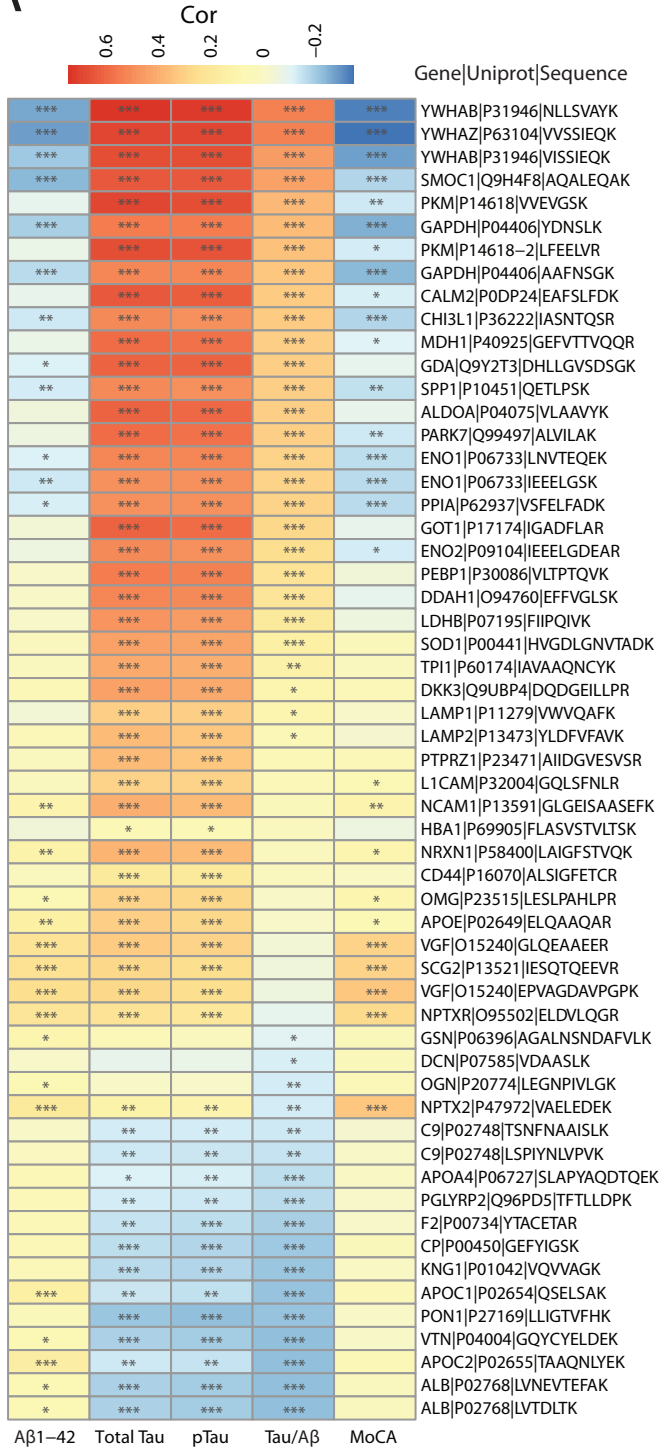


AsymAD-Control AD-Control AD-AsymAD

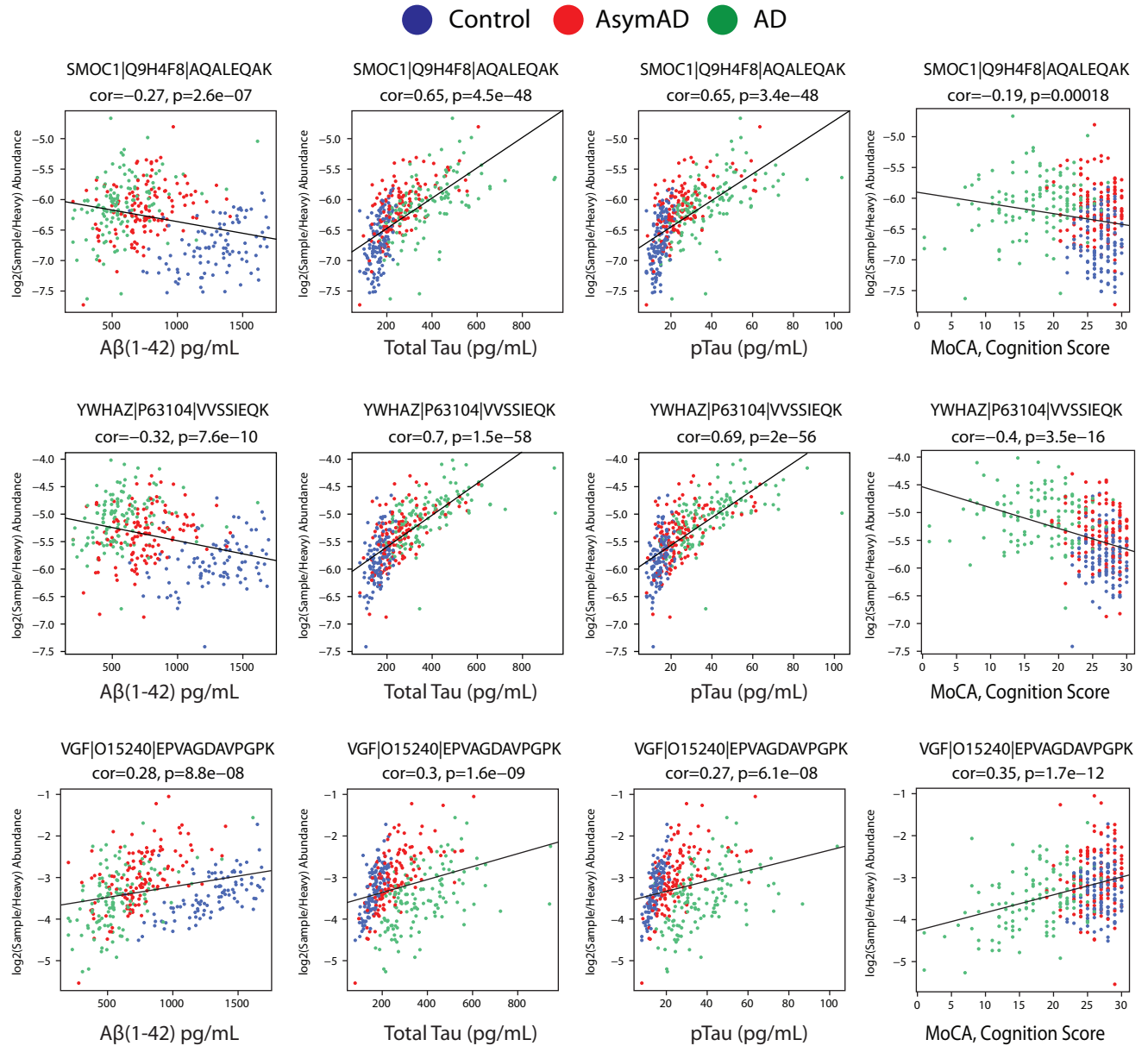
B

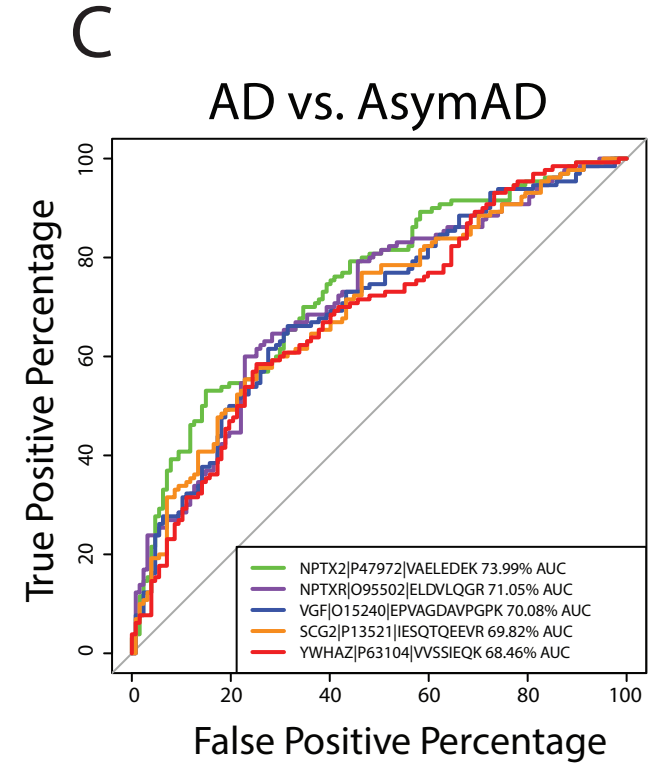
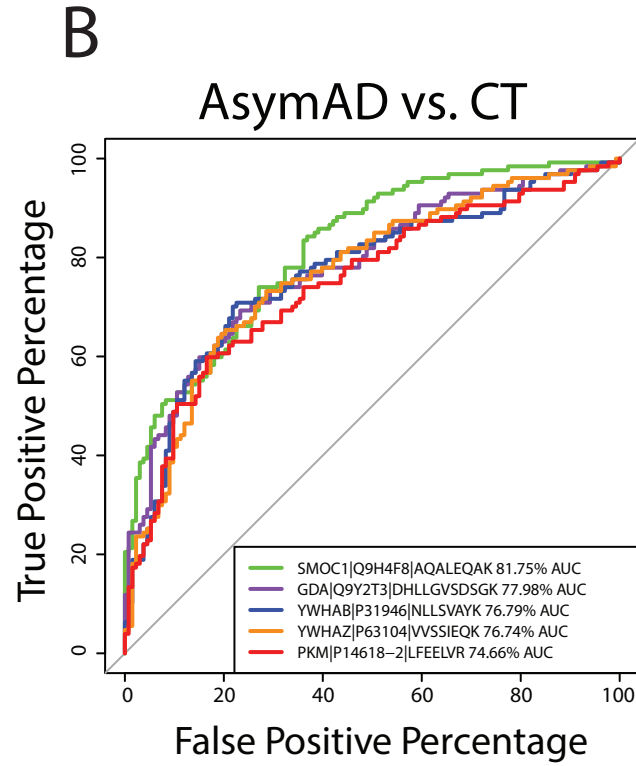
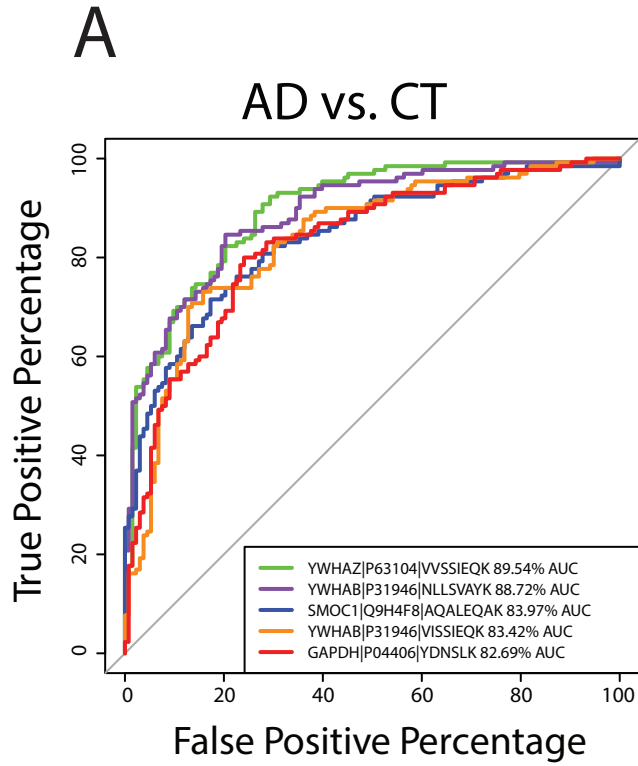


A



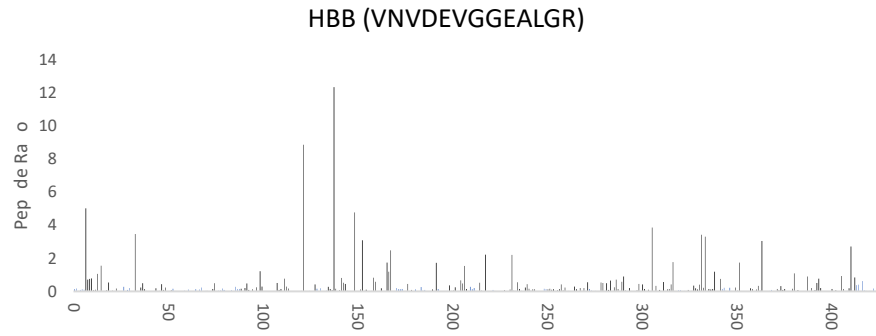
B



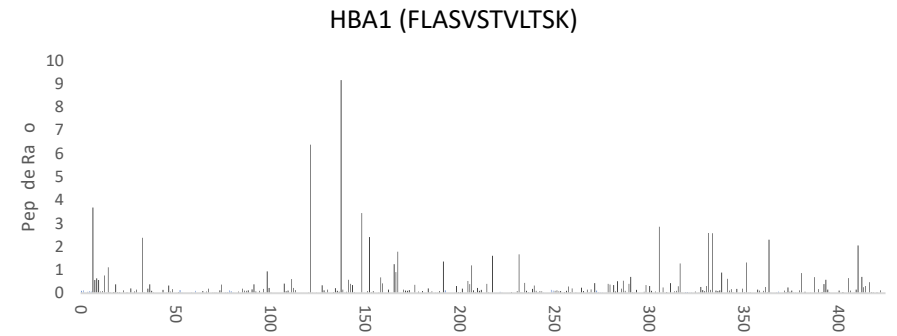


# Supplemental Figure 1

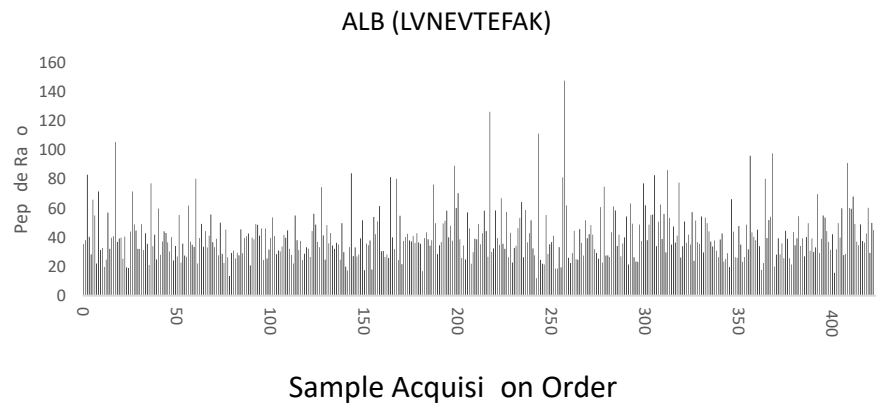
## A



## B



## C



## D

